ACS APPLIED MATERIALS & INTERFACES

Research Article

www.acsami.org

Multilayer Capsules of Bovine Serum Albumin and Tannic Acid for Controlled Release by Enzymatic Degradation

Maria V. Lomova,[†,‡,§] Anna I. Brichkina,[∥] Maxim V. Kiryukhin,[‡] Elena N. Vasina,[∥] Anton M. Pavlov,[†,§] Dmitry A. Gorin,[†] Gleb B. Sukhorukov,[§] and Maria N. Antipina*[,‡]

[†]Saratov State University, 83 Astrakhanskaya Street, Saratov, 410012, Russia

[‡]Institute of Materials Research and Engineering, A*STAR (Agency for Science, Technology and Research), 3 Research Link, Singapore 117602, Singapore

[§]School of Engineering and Materials Science, Queen Mary University of London, Mile End Road, London E1 4NS, United Kingdom

[∥]Institute of Molecular and Cell Biology A*STAR (Agency for Science, Technology and Research), 61 Biopolis Drive, Proteos, Singapore 138673, Singapore

Supporting Information

ABSTRACT: With the purpose to replace expensive and significantly cytotoxic positively charged polypeptides in biodegradable capsules formed via Layer-by-Layer (LbL) assembly, multilayers of bovine serum albumin (BSA) and tannic acid (TA) are obtained and employed for encapsulation and release of model drugs with different solubility in water: hydrophilic-tetramethylrhodamine-isothiocyanate-labeled BSA (TRITC-BSA) and hydrophobic 3,4,9,10-tetra-(hectoxy-carbonyl)-perylene (THCP). Hydrogen bonding is proposed to be predominant within thus formed BSA/TA films. The TRITC-BSA-loaded capsules comprising 6 bilayers of the protein and polyphenol are benchmarked against the shells composed of dextran sulfate (DS) and poly-L-arginine (PARG) on degradability by two proteolytic enzymes with different cleavage site specificity (i.e., α-chymotrypsin and trypsin) and toxicity for murine RAW264.7 macrophage cells. Capsules of both types possess low cytotoxicity taken at concentrations equal or below 50 capsules per cell, and evident susceptibility to α-chymotrypsin resulted in release of TRITC-BSA. While the BSA/TA-based capsules clearly display resistance to treatment with trypsin, the assemblies of DS/PARG extensively degrade. Successful encapsulation of THCP in the TRITC-BSA/TA/BSA multilayer is confirmed, and the release of the model drug is observed in response to treatment with α-chymotrypsin. The thickness, surface morphology, and enzyme-catalyzed degradation process of the BSA/TA-based films are investigated on a planar multilayer comprising 40 bilayers of the protein and polyphenol deposited on a silicon wafer. The developed BSA/TA-based capsules with a protease-specific degradation mechanism are proposed to find applications in personal care, pharmacology, and the development of drug delivery systems including those intravenous injectable and having site-specific release capability.

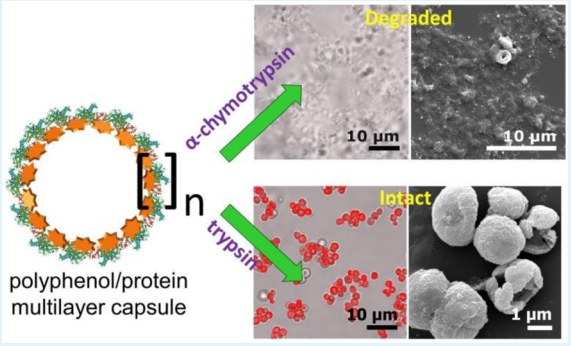

KEYWORDS: *layer-by-layer, encapsulation, protein, tannic acid, enzymatic degradation, controlled release*

INTRODUCTION

In situ release of active molecules in response to external stimuli is one of the key features of smart nano- and micron-sized encapsulating systems. Although drug delivery remains the main application area, these systems can be found nowadays in food and feed, functional coatings, personal care, laundry, and home care products.

Layer-by-layer (LbL) assembled polymer composite microcapsules are proven to be prospective for various application areas due to versatility with respect to payload, targeted delivery, and controlled release options. LbL shells can retain a variety of molecules and other payload with different water solubility and perform either gradual release by diffusion or burst release forced by remote activation with light, magnetic field, ultrasound, temperature, pH, salinity, redox potential, and chemicals.[1−4] The development of capsules decomposing in response to biological stimuli, such as enzymatic cleavage, is of particular significance for biomedicine, personal care, and food industries. Enzymatically degradable capsules made of oppositely charged polypeptides[5] or polysaccharide-coupled polyamino acids[6] have been extensively investigated with the scope of retention and release of water-soluble macromolecules[7] and employed for delivery of genes,[8,9] growth factors,[10,11] and vaccines.[12−14] The main drawback of the above-mentioned capsules is the use of expensive and significantly cytotoxic polycations that limits their practical

Received: October 22, 2014
Accepted: May 19, 2015
Published: May 19, 2015

DOI: 10.1021/acsami.5b03263
ACS Appl. Mater. Interfaces 2015, 7, 11732−11740

application. Unmodified chitosan is one candidate among a group of very few cheap alternatives to polyamino acids in electrostatically driven multilayer assemblies. However, chitosan possesses good solubility in water only at acidic pH[15,16] and may not be suitable for encapsulation of pH sensitive payload. Moreover, chitosan and its modifications are yet to receive FDA approval for health-related applications.

Interfacial complexation of macromolecules via hydrogen bonding[17,18] allows the production of capsules without using polycations.[19−21] Tannic acid (TA), a plant polyphenol of natural origin, is a quite popular building block in such assemblies.[17−19,21,22]

Protein-based drugs are essential components of medical care, and for that reason, protein layered films were studied as early as in the 1990s,[23] almost immediately after the LbL method for polyelectrolytes was published for the first time by Decher and co-workers.[24] The ability of tannins and other polyphenols to precipitate proteins from solution[25] turns out to be an easy way to include proteins in LbL films and encapsulating shells. Polyphenols benefit the assemblies through enhancing the protein stability by their antioxidant activity[26−33] and UV-absorbing properties.[33] In addition, thermally stable proteins are often used for encapsulation of those polyphenols sensitive to high temperature and oxidation.[34,35] Proteases found inside the biological cells and digestive tracts of living organisms can cleave the peptide bonds of protein building blocks in the protein/polyphenol films, thereby disrupting the complex. Therefore, capsules made of protein/polyphenol multilayers are envisioned to possess the enhanced stability of both ingredients and enzymatically triggered degradation mechanism essential for in situ intracellular delivery and oral administration of drugs and active compounds.

Protein/polyphenol complexes are most frequently based on hydrophobic interactions[36] and hydrogen bonding,[37] although in the case of positively charged polyamino acids (poly-L-arginine and poly-L-lysine), the reaction is predominantly electrostatic.[38] The phenolic group is an excellent hydrogen donor forming hydrogen bonds with the protein's carboxyl group that are stronger than hydrophobic interactions at normal temperatures and low ionic strength.[36] In consistence, the reaction of tannic acid with an immobilized layer of bovine serum albumin (BSA) was mainly hydrogen bonding,[39] despite ca. 46% of hydrophobic amino acids present in the protein structure according to Stein et al.[40] Hydrophobic interactions of protein and polyphenol can nevertheless be strong enough to form free-standing capsules, as it has been shown for proline-enriched gelatin coupled with (−)-epigallocatechin gallate.[41] Although these capsules, with no electrostatic forces contributing to interlayer interactions, were observed having severe structural defects.[41]

This work is devoted to the fabrication of capsules composed of bovine serum albumin and tannic acid with a potential for controlled enzyme-catalyzed release of molecules with different solubility in water. BSA was chosen as one of the shell constituents because of its availability, good water solubility over a wide range of pH values, and low cost with respect to commonly used polyamino acids. The BSA/TA complexes in the bulk phase have been extensively studied elsewhere.[42,43] Recently, we have demonstrated stabilization of a fragrance containing oil-in-water emulsions with BSA/TA layers.[44] However, the possibility to obtain hollow capsules and encapsulation of water-soluble molecules are yet to be discovered. Here, the BSA/TA multilayers are employed to encapsulate a water-soluble model drug, tetramethylrhodamine-isothiocyanate-labeled BSA, and a hydrophobic model drug, 3,4,9,10-tetra-(hectoxy-carbonyl)-perylene). Then the capsule degradation is studied under the effect of two proteolytic enzymes with different cleavage site specificity (i.e., α-chymotrypsin and trypsin). To confirm that the obtained BSA/TA-based capsules are suitable for biorelated applications, their cytotoxicity is studied and benchmarked against the poly-L-arginine/dextran sulfate multilayer assembly previously reported for intracellular drug delivery.[6,12] The thickness and morphology of the BSA/TA-based multilayer film are investigated by means of scanning electron microscopy and atomic force microscopy of the multilayers deposited on a flat solid substrate.

EXPERIMENTAL SECTION

Materials. Dextran sulfate, sodium salt (Dex, MW > 500 000), poly-L-arginine hydrochloride (PARG, MW > 70 000), bovine serum albumin (BSA), tetramethylrhodamine-isothiocyanate-labeled bovine serum albumin (TRITC-BSA), α-chymotrypsin from bovine pancreas (98.7 U/mg, ≥ 40 units/mg protein), trypsin from bovine pancreas (≥10.000 units/mg protein), polyethylenimine (branched, average MW ∼25.000) (PEI), tannic acid (TA), boric acid, hydrochloric acid, calcium chloride dihydrate, anhydrous sodium carbonate, ethylenediaminetetraacetic acid trisodium salt (EDTA), sunflower oil, and *In Vitro* Toxicology Assay Kit (3-(4,5-dimethylthiazol-2-yl)-2,5-diphenyltetrazolium bromide (MTT) based) were obtained from Sigma-Aldrich, and dimethyl sulfoxide (DMSO) and hydrochloric acid were obtained from Merck and used without further purification. 3,4,9,10-Tetra-(hectoxy-carbonyl)-perylene (THCP) was synthesized as described elsewhere.[45] Deionized water with specific resistivity higher than 18.2 MΩcm from a three-stage Milli-Q Plus 185 purification system was used in the experiments. Single-side-polished boron-doped Prime silicon wafers (675 μm thick) were purchased from Syst Integration Pte Ltd. (Singapore).

Preparation of TRITC-BSA-Loaded Microcapsules. BSA/TA-based capsules loaded with a model water-soluble active compound, TRITC-BSA, were prepared with assistance of a $CaCO_3$ sacrificial template, as depicted in Figure 1a. $CaCO_3$ microparticles were synthesized according to Volodkin et al.[46] In brief, TRITC-BSA (2 mL, 0.8 mg/mL in water) was successively mixed with equivalent amounts of $CaCl_2$ and Na_2CO_3 solutions (0.615 mL, 1 M) under vigorous agitation. Spherical TRITC-BSA loaded $CaCO_3$ particles with an average diameter of 3 μm were then collected by centrifugation and washed with water. To ensure good mechanical stability of the forming capsules, a 2 mg/mL PARG solution in 0.5 M NaCl was used to form the first layer. A multilayer shell comprising six bilayers of TA/BSA was then assembled in the LbL fashion alternately using 3 mg/mL solution of TA (pH 3) and 4 mg/mL solution of BSA (pH 5.8) with two washing steps after deposition of each layer. This procedure was repeated six times resulting in six deposited bilayers. Two consecutive treatments with 0.2 M EDTA lasting for 15 min each were then performed to extract $CaCO_3$. Beforehand, pH in the EDTA solution was adjusted to 7.0 by 1 M HCl. Similar to polymeric multilayer capsules of other biodegradable constituents, PARG/$[DS/PARG]_6$ has good structural stability and is not prone to aggregate upon storage at 4 °C. The stability studies are presented in Figure S1, Supporting Information.

PARG/$[DS/PARG]_6$ capsules were fabricated in the same manner using 2 mg/mL aqueous solutions of respective polymers also containing 0.5 M NaCl.

Encapsulation of THCP. Encapsulation of THCP was carried as it schematically shown in Figure 1b via slightly modified routine described previously by our group.[47,48] In brief, 10 000 ppm of THCP dissolved in 1 mL of sunflower oil was added to 9 mL of a 4 mg/mL TRITC-BSA aqueous solution and shaken in a 50 mL centrifuge tube for 10 s. The suspension was then homogenized for 2

DOI: 10.1021/acsami.5b03263
ACS Appl. Mater. Interfaces 2015, 7, 11732−11740

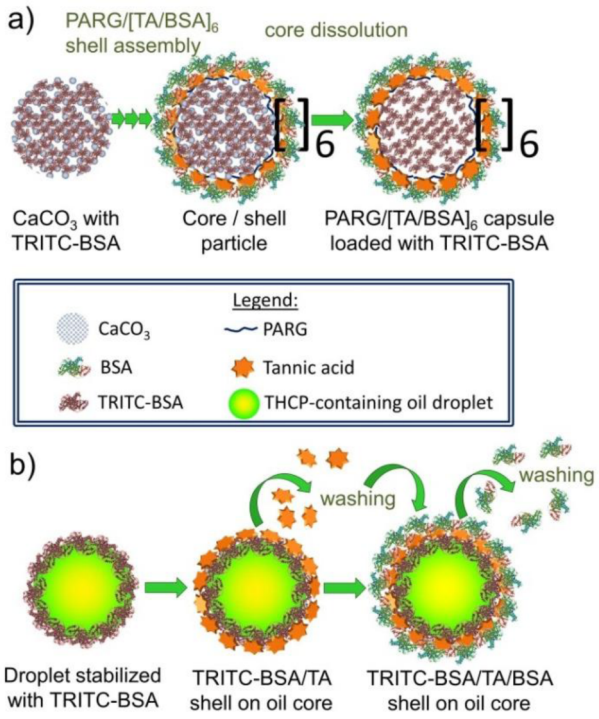

Figure 1. Schematic representation of encapsulation of model drugs with different solubility in water in protein/polyphenol assemblies. Encapsulation of TRITC-BSA (a) and THCP (b).

min by an Ultra Turrax disperser (IKA, Germany) at 24 000 rpm and allowed to relax for 15 min. After adding of 20 mL of TA solution, the suspension was again treated by the Ultra Turrax disperser for 1 min and then transferred to a 50 mL stirred filtration cell (Millipore Corp., U.S.A.) and kept under vigorous agitation for 15 min followed by three washing cycles. To adsorb an outmost layer of BSA, 10 mL of filtered suspension was covered with 20 mL of a 2 mg/mL BSA solution and stirred for 15 min also followed by three washing cycles. The obtained capsules are stable upon long-term storage at 4 °C.[44]

Assembly of a BSA/TA Multilayer Film on a Flat Substrate. LbL assembly on flat silicon wafers (2 × 3 cm) was performed by a dipping method comprising deposition steps lasting for 10 min followed by thorough rinsing the wafers with water.[49,50] The wafers were first subjected to RCA-1 cleaning[51] and coated with an anchor layer of PEI deposited from its aqueous solution (2 mg/mL, 2 M NaCl). Alternate adsorption of BSA and TA was then performed using their respective 4 and 3 mg/mL water solutions. The resulting PEI/BSA/$[TA/BSA]_{40}$ film was dried in air at room temperature.

Enzymatic Treatment. To provide optimal operating pH, borate buffer (0.1 M, pH 8.0) and phosphate buffered saline (1 ×, pH 7.4) were chosen to prepare solutions of trypsin and α-chymotrypsin, respectively. Freshly prepared PARG/$[DS/PARG]_6$ and PARG/$[TA/BSA]_6$ microcapsules were first transferred into the respective buffers, and then 100 μL of each suspension containing ca. 1.5% v/v of capsules were mixed with the corresponding enzyme solution (V = 250 μL) containing 2 kU of the enzyme. The mixtures were placed in 2 mL centrifuge tubes and kept at 37 °C for 10 h. α-Chymotrypsin treatment of the TRITC-BSA/TA/BSA shells encapsulating THCP was performed in a similar manner visualizing the results after 12 h.

Planar silicon wafers coated with PEI/BSA/$[TA/BSA]_{40}$ layers were immersed into 1 mL of α-chymotrypsin solutions with different concentrations of the enzyme (0.002 mg/mL, 0.02 mg/mL, and 0.2 mg/mL equal to 0.197 U, 1.97 U and 19.7 U respectively) for 1 min at 37 °C followed by drying the wafers in air at room temperature before further analysis.

Characterization. The capsules and films were analyzed with Atomic Force Microscopy (AFM), Confocal Laser Scanning Microscopy (CLSM), and Scanning Electron Microscopy (SEM). Cell viability was obtained via MTT assay. The detailed description of the analytical methods and characterization tools used in the manuscript is available as Characterization, Supporting Information.

RESULTS AND DISCUSSION

Encapsulation and Enzyme-Catalyzed Release of TRITC-BSA. It was mentioned that the shells formed of solely BSA/TA multilayers decomposed upon extraction of $CaCO_3$, but the respective capsules possessed good mechanical stability, if an anchor layer of a TA-binding polycation was adsorbed on the surface of $CaCO_3$. For consistency, PARG was chosen to form an anchor layer in the BSA/TA-based capsules in our experiments. Adsorption of a layer of TA on TRITC-BSA-containing $CaCO_3$ precipitate coated with a layer of PARG resulted in microparticles having a bluish-green tint that gradually became more intense upon deposition of the consequent layers of TA. The particle color change was not observed for the PARG/DS pair and could be caused by oxidation of TA, which is known to happen in solutions with pH > 7 due to reaction with atmospheric oxygen.[18] To investigate the mechanism of the protein/polyphenol multilayer assembly on the surface of $CaCO_3$ precipitate, pH in the continuous phase was measured in each step of the capsule formation process (Figure 2).

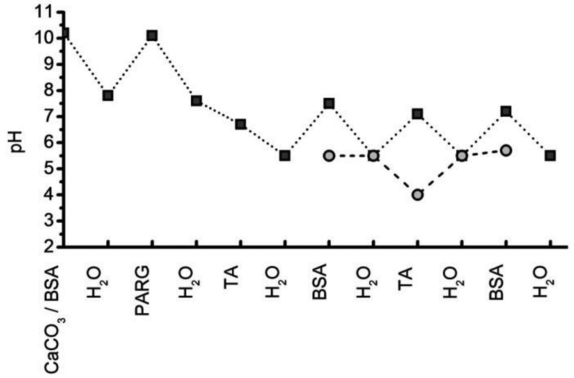

Figure 2. Continuous phase pH upon the protein/polyphenol film assembly on the surface of TRITC-BSA-loaded $CaCO_3$ (··■··), water-dispersed THCP microdroplets (gray --●--).

Mixing the equivalent volumes of 1 M $CaCl_2$ and Na_2CO_3 aqueous solutions results in precipitation of vaterite, which is a metastable polymorph of calcium carbonate characterized by spherical shape, micrometer size, high porosity, and higher water solubility if compared to calcite or aragonite.[52] If formed in the presence of macromolecules (like, for instance, TRITC-BSA used in our experiments), they will be absorbed by growing porous particles.[46] pH in the solution after calcium carbonate precipitation was ~10 (Figure 2) due to relatively high saturation concentration of sodium carbonate. Upon further washing of the precipitate with water, the solution pH dropped but remained slightly alkaline at 7.5. This pH well above the isoelectric point of BSA (4.7) ensured a negative surface charge of calcium carbonate microparticles. Further introduction of PARG aqueous solution (2 mg/mL, pH 5.5) resulted in immediate increase of pH back to highly alkaline value of ~10. The reason could be that the adsorption of the polycation on calcium carbonate was accompanied by complexation of Ca^{2+} with guanidinium and peptide nitrogens of PARG,[53] partial dissolution of calcium carbonate, and release of

DOI: 10.1021/acsami.5b03263
ACS Appl. Mater. Interfaces 2015, 7, 11732−11740

sodium carbonate. Washing with water reduced pH back to slightly alkaline value of 7.5. When TA was introduced to $CaCO_3$/TRITC-BSA/PARG precipitate, the continuous phase pH increased to ~7. TA is a very weak acid with pK_a ~ 8.5, but its solution has a rather low pH of ~3, possibly reflecting natural acidity of the tannin extract[54] and hydrolysis of tannic acid with formation of gallic acid.[55] Again, the reason for the pH increase in this step could be partial dissolution of $CaCO_3$ and additional complexing of Ca^{2+} ions with tannic acid or the products of its hydrolysis. Such complexes are known to be insoluble in water and could coexist with $CaCO_3$/TRITC-BSA/PARG/TA microparticles.[54] This trend was followed upon further process of multilayer assembly: washing with water reduced pH to ~5.5 but introduction of BSA or TA increased pH back to ~7 (Figure 2). pK_a of TA (~8.5), literature data,[36,37,39] and the results in Figure 2 allow us to propose hydrogen bonding as the predominant type of interlayer interactions within the formed BSA/TA-based multilayer shell. Because hydrogen bonding is the most likely to be involved in the complex formation, the coupling molecules of BSA might undergo the conformation changes. A better understanding of the molecular conformation would require X-ray analysis that is beyond the scope of this manuscript.

$CaCO_3$ extraction by EDTA entailed with extensive burst release of the colored complex. It means that the oxidized form of TA mainly presented in TA-Ca^{2+} insoluble complexes but not in the PARG/$[TA/BSA]_6$ capsules. The complex was dissolved by EDTA, and the products were washed away upon further washing steps. However, the resulted pellet of the PARG/$[TA/BSA]_6$ capsules still had a darker shade than that of the PARG/$[DS/PARG]_6$ composition.

The obtained PARG/$[TA/BSA]_6$ and PARG/$[DS/PARG]_6$ capsules were treated by two proteolytic enzymes (α-chymotrypsin and trypsin), with the aim to compare their degradation properties. The results of microscopy studies of freshly prepared PARG/$[TA/BSA]_6$ and PARG/$[DS/PARG]_6$ capsules are shown in the top section of Figure 3. CLSM evidence successful formation of the protein/poly phenol microcapsules. In addition, the SEM image displays that these capsules were not collapsed and significantly denser than their counterparts. Immediately performed EDX measurements (Figure S2, Supporting Information) confirmed complete decomposition of the $CaCO_3$ template, so that the observed morphology was proven attributed to the protein/polyphenol multilayers rather than being a result of the incomplete core extraction.

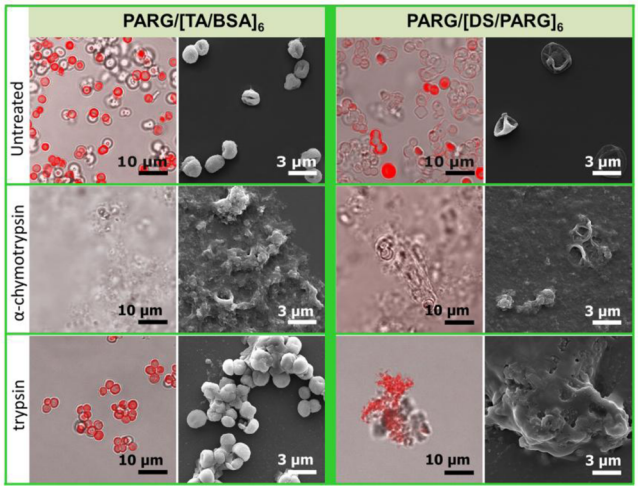

Figure 3. Representative CLSM and SEM images of the PARG/$[TA/BSA]_6$ and PARG/$[DS/PARG]_6$ capsules before (top section) and after their 10 h treatment with α-chymotrypsin (middle section) and trypsin (bottom section).

CLSM and SEM images taken after 10 h of incubation with α-chymotrypsin (Figure 3, middle section) evidence that the capsules of both types were destroyed. The fluorescent signal of the encapsulated TRITC-BSA disappeared, indicating the protein was released from the capsules and most likely was degraded by the enzyme later. A minor amount of intact-looking shells of both types were also observed in the respective batches (Figure S3, Supporting Information) probably evidencing the enzyme aging that happens faster than in 10 h. Another possible explanation is that these capsules initially occurred inside larger aggregates, and became covered by nondegradable shell residues of their outer neighbors. The structures resembling not fully decomposed capsules were seen more often in the sample of DS/PARG-based formulation (Figure S3, Supporting Information).

It is important to highlight that the enzyme-catalyzed degradation of the protein/polyphenol capsules was observed only when their outmost layer was formed by BSA. A possible reason could be precipitation of the α-chymotrypsin molecules by the molecules of TA at the capsule surface causing the protease to deactivate. Indeed, extensive turbidity seen upon mixing of solutions of TA and α-chymotrypsin in a test tube supports this assumption.

PARG/$[TA/BSA]_6$ shells preserved their integrity and did not release payload in trypsin solution. The CLSM image in Figure 3 bottom section left displays undistorted spherical shape of these capsules and strong intensity of fluorescence of the encapsulated TRITC-BSA. A minor impact of the trypsin treatment is seen in appearance of small aggregates, which might also be an issue of a higher storage temperature. Indeed, PARG/$[TA/BSA]_6$ capsules were noted to form small aggregates even in pure water if stored at 37 °C for 10 h. In agreement, the respective SEM image in Figure 3 confirms integrity of the protein/polyphenol multilayers. Some amount of broken capsules seen by SEM might be also a result of the temperature regime rather than being caused by enzymatic activity. Several probes of the respective sample were thoroughly analyzed with no differences in the capsule integrity noticed (Figure S4, Supporting Information).

The observed results can be explained by a different cleavage site specificity of α-chymotrypsin and trypsin. α-Chymotrypsin hydrolyzes amide bonds at the sites of various amino acids but preferentially cleaves peptide amide bonds where the carboxyl side of the amide bond is a large hydrophobic amino acid (tyrosine, tryptophan, or phenylalanine). BSA contains 6.56% of phenylalanine, 5.06% of tyrosine, and 0.58% of tryptophan,[40] which sites were supposed to be actively cleaved by the enzyme within the structure of the PARG/$[TA/BSA]_6$ capsules. The fact that the PARG/$[DS/PARG]_6$ capsules were also degraded by α-chymotrypsin is hence an evidence of a sufficient unspecific activity of this enzyme toward the amide bonds in PARG.

Trypsin cleaves peptide chains mainly at the carboxyl side of the amino acids lysine or arginine. In agreement, the sites of arginine in the PARG/$[DS/PARG]_6$ capsules were subjected to cleavage by trypsin. Relatively low content of lysine and arginine in BSA is presumably the reason for the PARG/[TA/

DOI: 10.1021/acsami.5b03263
ACS Appl. Mater. Interfaces 2015, 7, 11732−11740

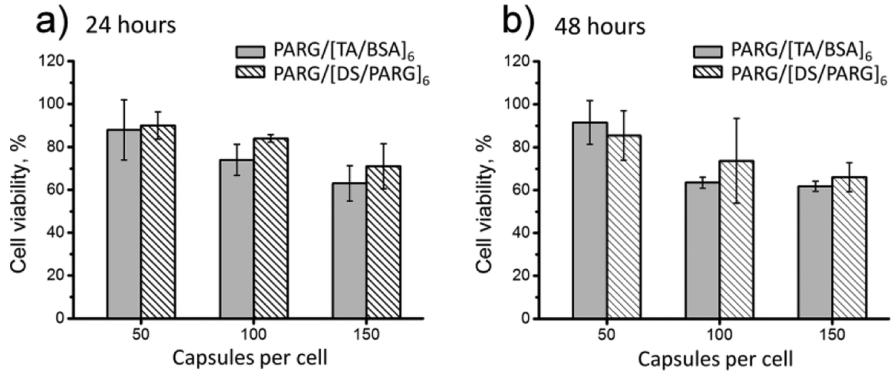

Figure 4. Murine RAW264.7 macrophage cell viability in the presence of PARG/$[TA/BSA]_6$ and PARG/$[DS/PARG]_6$ capsules after incubation for 24 h (a) and 48 h (b).

$BSA]_6$ shells were not susceptible to trypsin. Moreover, the fluorescence of the TRITS-BSA payload can be clearly seen by CLSM in the sample of the PARG/$[DS/PARG]_6$ capsules treated with trypsin, although the capsules themselves were fully decomposed by the enzyme, as suggested by both CLSM and SEM visualization methods (Figure 3 bottom section right). Indeed, the total amount of lysine and arginine in BSA is 18.72%;[40] however, this forms less than 9% of total amount of arginine monomers in PARG.

Because trypsin has been proved inactive toward BSA and its multilayer complex with polyphenol, the BSA/TA capsules could find application in pharmacology as a component of trypsin-based drug formulations. Strong selectivity toward different proteases seen for the protein/polyphenol capsules opens up an opportunity to develop delivery systems with a site-specific release mechanism.

Cell Viability. PARG/DS shells of different thickness have been already found possessing low cytotoxicity for L929 cell line.[11] Thus, the protein/polyphenol microcapsules, PARG/$[TA/BSA]_6$, were benchmarked against the PARG/$[DS/PARG]_6$ counterparts regarding the effect on viability of murine RAW264.7 macrophage cells.

For cytotoxicity studies, murine RAW264.7 macrophage cells were cultured for 48 h in the presence of PARG/$[TA/BSA]_6$ or PARG/$[DS/PARG]_6$ capsules. Both investigated compositions evidently possess low cytotoxicity at concentrations equal or below 100 capsules/cell during the first 24 h (Figure 4a). However, after the next 24 h, the MTT assay revealed for both that the cell viability dropped below 80% for concentrations of 100 capsules/cell and 150 capsules/cell (Figure 4b). Therefore, 50 capsules/cell represents the concentration at which both PARG/$[TA/BSA]_6$ and PARG/$[DS/PARG]_6$ capsule compositions have no major negative effect on cell viability.

As for toxicity of TRITC-BSA/TA/BSA shells, which were used below in the manuscript to encapsulate THCP, it is expected to be even less compare to that of PARG/$[TA/BSA]_6$ because of smaller total amount of the shell constituents and the complete absence of polycation. Unfortunately, creaming (due to the gravitational oil/water separation) makes this sample inappropriate for cell culture study to verify the presumption.

Murine RAW264.7 macrophages were also cultured in the presence of a sole component of each of the investigated compositions monitoring the cell viability after 24 and 48 h of incubation (Figure S5, Supporting Information). Whereas BSA, TA, and DS appear noncytotoxic within the concentration interval from 1×10^{-2} to 3×10^{-2} mg/mL, drastic inhibition of the cell proliferation was detected for PARG at the 48 h time point, presumably due to the polymer interacting with the oppositely charged membranes of the macrophages affecting their growth. This result clearly suggests the potential benefit of exploiting the TA/BSA-based capsules in biomedical applications as they contain no apparent cytotoxic polycations.

Encapsulation and Release of THCP. TRITC-BSA stabilized THCP microdroplets were characterized with negative ζ-potential of (-18 ± 1.8) mV, which should correspond to the continuous phase pH slightly above the isoelectric point of the protein (4.7). In consistence, pH in the continuous phase appeared to be 5.5 (Figure 2). After the microdroplets were immersed into the solution of TA, pH dropped down to 4, and ζ-potential remained almost unchanged ((-16 ± 3) mV). It is worthwhile to note that the continuous phase pH in this case was drastically lower than during the BSA-TA shell assembly on $CaCO_3$ particles. It confirms our hypothesis that high pH in the previous case was due to $CaCO_3$ dissolution upon Ca^{2+} complexing with TA and formation of sodium carbonate. Adsorption of the consequent layer of unlabeled BSA resulted in the particle surface charge of (-30 ± 1.9) mV and pH of the continuous phase of 5.7. Negative values of ζ-potential upon shell assembly allow us to exclude contribution of electrostatic forces also proposing hydrogen bonding between the layers. It could be mentioned that pH in the continuous phase did not drop below 4 over the whole encapsulation process and was above 5 when BSA was introduced to form a consequent layer (Figure 2). According to Barbosa et al., these observations allow the expectation that there are no significant conformational changes in the protein structure caused by pH.[56]

THCP-containing oil microdroplets prepared as described above have been previously characterized with a broad size distribution and the mean diameter of (3.8 ± 0.8) μm.[44] Microdroplets larger than 2 μm can be well resolved by a confocal microscope. CLSM images of the protein/polyphenol shells, TRITC-BSA/TA/BSA, encapsulating THCP are shown in Figure 5a. The microdroplets prominently display a core/shell structure visualized by green spots attributed to the THCP-containing oil cores (Figure 5a, top-left) and red surrounding circles attributed to the shells with a layer of TRITC-BSA (Figure 5a, bottom-left). The fluorescent (top-left and bottom-left), bright-field (top-right), and overlay (bottom-right) images in Figure 5a indicate that the cores and shells are colocalized giving an evidence of successful encapsulation of THCP-containing oil.

DOI: 10.1021/acsami.5b03263
ACS Appl. Mater. Interfaces 2015, 7, 11732−11740

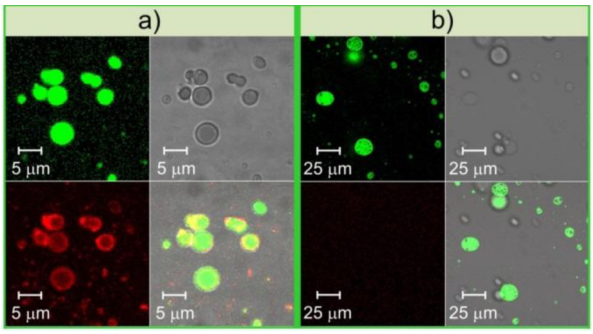

Figure 5. CLSM images of TRITC-BSA/TA/BSA coated oil microdroplets containing THCP before (a) and after (b) treatment with α-chymotrypsin for 10 h. In each pattern (a) and (b), top-left image is obtained at λ_{exc} = 488 nm, λ_{em} = 525 nm; bottom-left image is obtained at λ_{exc} = 529 nm, λ_{em} = 596 nm; top-right image is a bright-field microscopy image; bottom-right image is an overlay of top-left, bottom-left, and top-right images.

Among the two enzymes studied with respect to degradation of the PARG/$[TA/PARG]_6$ capsules loaded with TRITC-BSA, only α-chymotrypsin has shown decomposition activity. Because of this result, only α-chymotrypsin was used to initiate release of encapsulated THCP from the TRITC-BSA/TA/BSA shells. Incubation with α-chymotrypsin resulted in complete degradation of the particle shell and release of THCP. Indeed, CLSM images taken after the treatment with α-chymotrypsin display no signal from TRITC-BSA (Figure 5b, bottom-left). In addition, CLSM reveals extensive coalescence of THCP-containing oil droplets in response to the capsule decomposition by visualizing green spots of a significantly larger size than before the enzymatic treatment (Figure 5b, top-left and bottom-right). As seen in Figure 5, the α-chymotrypsin-treated THCP-containing oil droplets are approximately 5 times larger than the biggest particle captured in a freshly prepared sample. Similar to the BSA/TA-based capsules loaded with TRITC-BSA, the BSA/TA shells encapsulating droplets of THCP dissolved in oil remained intact upon treatment with α-chymotrypsin despite of their smaller thickness (data not shown).

BSA/TA Film Characterization. To characterize the BSA/TA film thickness and morphology, 40 respective bilayers were deposited on planar silicon wafers precoated with PEI followed by visualization by SEM and AFM. An SEM image of the film cross-section shown in Figure 6 displays areas with apparent height differences. The average thickness of the film was roughly measured to be 313 nm. The value reveals one bilayer

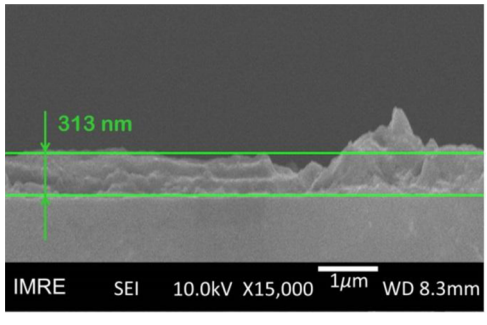

Figure 6. SEM image of the PEI/BSA/$[TA/BSA]_{40}$ film assembled on a flat silicon wafer.

of the BSA/TA-based film has a 7.8 nm thickness, which is in a good agreement with 6–8 nm obtained by quartz crystal microbalance technique for bilayers of (−)-Epigallocatechin gallate/type B gelatin coupled solely by hydrophobic interactions.[41]

AFM images in taping mode allow easy recognition of the area of interest as they provide high contrast of surface features located virtually at any height imaged. AFM amplitude imaging of the dried PEI/BSA/$[TA/BSA]_{40}$ film surface also evidence its considerable lateral inhomogeneity (Figure 7a) with numerous clusters of a 60–120 nm diameter.

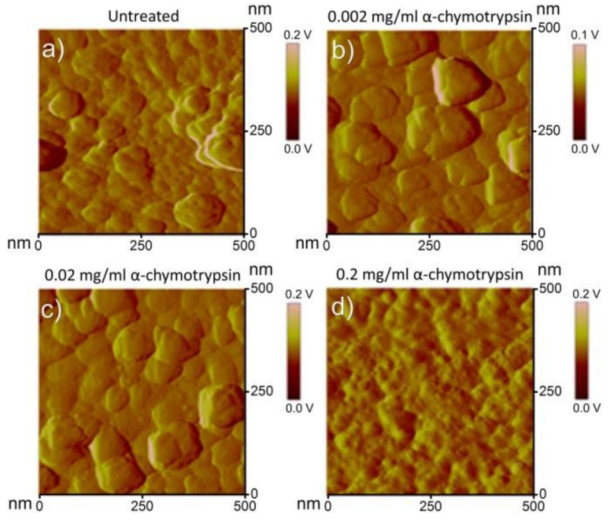

Figure 7. AFM amplitude images of the PEI/BSA/$[TA/BSA]_{40}$ film on a flat silicon wafer (a), after 1 min treatment with α-chymotrypsin solution with different concentrations of the enzyme: 0.002 mg/mL (b), 0.02 mg/mL (c), 0.2 mg/mL (d).

Treatment with 2 mg/mL solution of α-chymotrypsin over 5 min completely erased the film from the wafer surface. Thus, a series of experiments comprising treatments at several lower concentrations of the enzyme in the range of 0.002–0.2 mg/mL over a shorter period of time (1 min) was preformed to monitor the film decomposition process.

Enzymatic treatment caused significant changes in the film surface roughness reflected by the amplitude images (Figure 7b–d) and Table 1. The clusters observed for the untreated

Table 1. Parameters of the PEI/BSA/$[TA/BSA]_{40}$ Film Treated with α-Chymotrypsin Solutions of Different Concentrations Calculated from Respective AFM Scans

concentration of α-chymotrypsin, mg/mL	roughness, nm
0 (untreated)	14.0 ± 1.3
0.002	11.0 ± 2.4
0.02	8.0 ± 1.5
0.2	4.0 ± 0.3

film became visibly broader when the enzyme concentration increased from 0.002 mg/mL to 0.02 mg/mL (Figure 7b,c) and were erased in 0.2 mg/mL α-chymotrypsin solution followed by formation of small granular-like aggregates with a diameter of 25–35 nm (Figure 7d).

Analysis of the corresponding height images (images not shown) displayed that film roughness dropped by over 70% (from (14.0 ± 1.4) nm to (4.0 ± 0.3) nm) after treatment with

DOI: 10.1021/acsami.5b03263
ACS Appl. Mater. Interfaces 2015, 7, 11732–11740

0.2 mg/mL α-chymotrypsin solution compare to the untreated film (Table 1). The results suggest the surface flattening by erasing of large clusters predominantly occurs in the early stage of the enzyme-catalyzed PEI/BSA/$[TA/BSA]_{40}$ film degradation process presumably because the protein substrate is more readily available for the enzyme at the sites of eminences.

CONCLUSION

Successful fabrication of multilayers of bovine serum albumin (BSA) and tannic acid (TA) was demonstrated proposing interlayer hydrogen bonding predominantly responsible for complexation between protein and polyphenol. The BSA/TA multilayers were applied for encapsulation and enzyme-catalyzed release of model hydrophilic and hydrophobic drugs, tetramethylrhodamine-isothiocyanate-labeled BSA and 3,4,9,10-tetra-(hectoxy-carbonyl)-perylene, respectively.

TA/BSA-based capsules assembled on $CaCO_3$ sacrificial microparticles were benchmarked against the DS/PARG-based combination on degradation by two proteolytic enzymes, α-chymotrypsin and trypsin. Although degradation of both PARG/$[TA/BSA]_6$ and PARG/$[DS/PARG]_6$ shells by α-chymotrypsin was observed, capsules of protein and polyphenol stayed almost intact in trypsin solution due to inactivity of trypsin toward BSA. Toxicity of the PARG/$[TA/BSA]_6$ and PARG/$[DS/PARG]_6$ capsules for murine RAW264.7 macrophage cells was found in the same range. Both TA and BSA, when solely added to the cell culture medium, had no negative effect on cell viability, whereas it was drastically decreased in the presence of PARG.

Oil-dissolved THCP was successfully encapsulated with the TRITC-BSA/TA/BSA layers and released after α-chymotrypsin-catalyzed degradation of the shell. It was generally noticed that degradation of the BSA/TA-based capsules happened only in the case when the outmost layer was formed by BSA.

The study of the surface morphology and enzyme-catalyzed decomposition process of the protein/polyphenol multilayers revealed high surface roughness of the film attributed to the presence of large clusters, which were erased during the early stage of enzymatic treatment.

In the current system, an anchor layer of polycation was indispensable to produce hollow capsules of BSA and polyphenol. Still, by using just one layer of PARG in the formulation, the total capsule material cost was already considerably decreased (by almost 7 times according to the pricelist of Sigma-Aldrich) compared to PARG/$[DS/PARG]_6$. Thus, the protein/polyphenol-based formulation has clear benefits for personal care applications where the use of expensive materials represents a major drawback. In the field of drug delivery, such formulations open up an opportunity of using patient blood serum proteins to create a capsule, thus eliminating the immune response and thrombosis. Besides, protease-specific degradation clearly determined for the protein/polyphenol-based capsules is an encouraging finding for further developments of drugs and sophisticated delivery system with site-specific release mechanism.

ASSOCIATED CONTENT

Supporting Information

Full description of analytical methods and characterization tools, stability studies of PARG/$[TA/BSA]_6$ capsules, EDX analysis of PARG/$[TA/BSA]_6$ on $CaCO_3$ and PARG/$[TA/BSA]_6$ hollow capsules after core extraction, CLSM and SEM images of the enzymatically treated PARG/$[TA/BSA]_6$ and PARG/$[DS/PARG]_6$ capsules at different sample sites, cell viability data in the sole presence of BSA, TA, PARG, and DS. The Supporting Information is available free of charge on the ACS Publications website at DOI: 10.1021/acsami.5b03263.

AUTHOR INFORMATION

Corresponding Author

*E-mail: antipinam@imre.a-star.edu.sg (M.N.A.).

Author Contributions

The manuscript was written through contributions of all authors. All authors have given approval to the final version of the manuscript.

Funding

The study was supported by A*STAR's Joint Council Project Grant (Project No. 14302FG090) and Russian Government Grant No. 14.Z50.31.0004 (M.V.L, A.M.P, D.A.G, and G.B.S).

Notes

The authors declare no competing financial interest.

ACKNOWLEDGMENTS

The financial support by the A*STAR Graduate Academy, Singapore (M.V.L) and Biotechnology and Biological Sciences Research Council, UK (A.V.P) are greatly acknowledged. The authors thank Dr. Song Hong Yan (IMRE, A*STAR, Singapore) for kindly providing 3,4,9,10-tetra-(hectoxy- carbonyl)-perylene and Ms. Lee Shu Ying (NUMI NUS, Singapore) for assistance in CLSM measurements.

ABBREVIATIONS

LbL, layer-by-Layer
BSA, bovine serum albumin
TRITC-BSA, tetramethylrhodamine-isothiocyanate-labeled bovine serum albumin
TA, tannic acid
THCP, 3,4,9,10-tetra-(hectoxy-carbonyl)-perylene
DS, dextran sulfate
PARG, poly-L-arginine
PEI, polyethylenimine
EDTA, ethylenediaminetetraacetic acid
MTT, 3-(4,5-dimethylthiazol-2-yl)-2,5-diphenyltetrazolium bromide
DMSO, dimethyl sulfoxide
AFM, atomic force microscopy
SEM scanning electron microscopy
EDX, energy-dispersive X-ray spectroscopy
CLSM, confocal laser scanning microscopy

REFERENCES

(1) De Geest, B. G.; Sanders, N. N.; Sukhorukov, G. B.; Demeester, J.; De Smedt, S. C. Release Mechanisms for Polyelectrolyte Capsules. *Chem. Soc. Rev.* **2007**, *36*, 636−649.

(2) De Cock, L. J.; De Koker, S.; De Geest, B. G.; Grooten, J.; Vervaet, C.; Remon, J. P.; Sukhorukov, G. B.; Antipina, M. N. Polymeric Multilayer Capsules in Drug Delivery. *Angew. Chem., Int. Ed.* **2010**, *49*, 6954−6973.

(3) Antipina, M. N.; Sukhorukov, G. B. Remote Control over Guidance and Release Properties of Composite Polyelectrolyte Based Capsules. *Adv. Drug Delivery Rev.* **2011**, *63*, 716−729.

(4) Delcea, M.; Moehwald, H.; Skirtach, A. G. Stimuli-Responsive LbL Capsules and Nanoshells for Drug Delivery. *Adv. Drug Delivery Rev.* **2011**, *63*, 730−747.

(5) Marchenko, I.; Yashchenok, A.; Borodina, T.; Bukreeva, T.; Konrad, M.; Möhwald, H.; Skirtach, A. Controlled Enzyme-Catalyzed

DOI: 10.1021/acsami.5b03263
ACS Appl. Mater. Interfaces 2015, 7, 11732−11740

Degradation of Polymeric Capsules Templated on $CaCO_3$: Influence of the Number of LbL Layers, Conditions of Degradation, and Disassembly of Multicompartments. *J. Controlled Release* **2012**, *162*, 599−605.
(6) De Geest, B. G.; Vandenbroucke, R. E.; Guenther, A. M.; Sukhorukov, G. B.; Hennink, W. E.; Sanders, N. N.; Demeester, J.; De Smedt, S. C. Intracellularly Degradable Polyelectrolyte Microcapsules. *Adv. Mater.* **2006**, *18*, 1005−1009.
(7) She, Z.; Antipina, M. N.; Li, J.; Sukhorukov, G. B. Mechanism of Protein Release from Polyelectrolyte Multilayer Microcapsules. *Biomacromolecules* **2010**, *11*, 1241−1247.
(8) Shchukin, D. G.; Patel, A. A.; Sukhorukov, G. B.; Lvov, Y. M. Nanoassembly of Biodegradable Microcapsules for DNA Encasing. *J. Am. Chem. Soc.* **2004**, *126*, 3374−3375.
(9) Borodina, T.; Markvicheva, E.; Kunizhev, S.; Moehwald, H.; Sukhorukov, G. B.; Kreft, O. Controlled Release of DNA from Self-Degrading Microcapsules. *Macromol. Rapid Commun.* **2007**, *28*, 1894−1899.
(10) De Cock, L. J.; De Wever, O.; Van Vlierberghe, S.; Vanderleyden, E.; Dubruel, P.; De Vos, F.; Vervaet, C.; Remon, J. P.; De Geest, B. G. Engineered $(hep/pARG)_2$polyelectrolyte Capsules for Sustained Release of Bioactive TGF-β1. *Soft Mater.* **2012**, *8*, 1146−1154.
(11) She, Z.; Wang, C.; Li, J.; Sukhorukov, G. B.; Antipina, M. N. Encapsulation of Basic Fibroblast Growth Factor by Polyelectrolyte Multilayer Microcapsules and Its Controlled Release for Enhancing Cell Proliferation. *Biomacromolecules* **2012**, *13*, 2174−2180.
(12) De Koker, S.; De Geest, B. G.; Singh, S. K.; De Rycke, R.; Naessens, T.; Van Kooyk, Y.; Demeester, J.; De Smedt, S. C.; Grooten, J. Polyelectrolyte Microcapsules as Antigen Delivery Vehicles To Dendritic Cells: Uptake, Processing, and Cross-Presentation of Encapsulated Antigens. *Angew. Chem., Int. Ed.* **2009**, *48*, 8485−8489.
(13) De Geest, B. G.; Willart, M. A.; Hammad, H.; Lambrecht, B. N.; Pollard, C.; Bogaert, P.; De Filette, M.; Saelens, X.; Vervaet, C.; Remon, J. P.; Grooten, J.; De Koker, S. Polymeric Multilayer Capsule-Mediated Vaccination Induces Protective Immunity Against Cancer and Viral Infection. *ACS Nano* **2012**, *6*, 2136−2149.
(14) De Koker, S.; Naessens, T.; De Geest, B. G.; Bogaert, P.; Demeester, J.; De Smedt, S.; Grooten, J. Biodegradable Polyelectrolyte Microcapsules: Antigen Delivery Tools with Th17 Skewing Activity after Pulmonary Delivery. *J. Immunol.* **2010**, *184*, 203−211.
(15) Takei, T.; Nakahara, H.; Ijima, H.; Kawakami, K. Synthesis of a Chitosan Derivative Soluble at Neutral pH and Gellable by Freeze−Thawing, and Its Application in Wound Care. *Acta Biomater.* **2012**, *8*, 686−693.
(16) Sobol, M.; Bartkowiak, A.; de Haan, B.; de Vos, P. Cytotoxicity Study of Novel Water-Soluble Chitosan Derivatives Applied as Membrane Material of Alginate Microcapsules. *J. Biomed. Mater. Res., Part A* **2013**, *101A*, 1907−1914.
(17) Sukhishvili, S. A.; Granick, S. Layered, Erasable, Ultrathin Polymer Films. *J. Am. Chem. Soc.* **2000**, *122*, 9550−9551.
(18) Erel-Unal, I.; Sukhishvili, S. Hydrogen-Bonded Multilayers of a Neutral Polymer and a Polyphenol. *Macromolecules* **2008**, *41*, 3962−3970.
(19) Driver, K.; Baco, S.; Khutoryanskiy, V. Hollow Capsules Formed in a Single Stage via Interfacial Hydrogen-Bonded Complexation of Methylcellulose with Poly(acrylic acid) and Tannic Acid. *Eur. Polym. J.* **2013**, *49*, 4249−4256.
(20) Kozlovskaya, V.; Sukhishvili, S. A. pH-Controlled Permeability of Layered Hydrogen-Bonded Polymer Capsules. *Macromolecules* **2006**, *39*, 5569−5572.
(21) Kozlovskaya, V.; Kharlampieva, E.; Drachuk, I.; Cheng, D.; Tsukruk, V. V. Responsive Microcapsule Reactors Based on Hydrogen-Bonded Tannic Acid Layer-by-Layer Assemblies. *Soft Matter.* **2010**, *6*, 3596−3608.
(22) Kozlovskaya, V.; Zavgorodnya, O.; Chen, Y.; Ellis, K.; Tse, H. M.; Cui, W. X.; Thompson, J. A.; Kharlampieva, E. Ultrathin Polymeric Coatings Based on Hydrogen-Bonded Polyphenol for Protection of Pancreatic Islet Cells. *Adv. Funct. Mater.* **2012**, *22*, 3389−3398.
(23) Lvov, Y.; Ariga, K.; Ichinose, I.; Kunitake, T. Assembly of Multicomponent Protein Films by Means of Electrostatic Layer-by-Layer Adsorption. *J. Am. Chem. Soc.* **1995**, *117*, 6117−6122.
(24) Decher, G.; Hong, J.-D.; Schmitt, J. Buildup of Ultrathin Multilayer Films by a Self-assembly Process: III. Consecutively Alternating Adsorption of Anionic and Cationic Polyelectrolytes on Charged Surfaces. *Thin Solid Films* **1992**, *210/211*, 831−835.
(25) Mehansho, H.; Butler, L. G.; Carlson, D. M. Dietary Tannins and Salivary Proline-rich Proteins: Interactions, Induction, and Defense Mechanisms. *Annu. Rev. Nutr.* **1987**, *7*, 423−440.
(26) Shutava, T. G.; Prouty, M. D.; Agabekov, V. E.; Lvov, Y. M. Antioxidant Properties of Layer-by-Layer Films on the Basis of Tannic Acid. *Chem. Lett.* **2006**, *35*, 1144−1145.
(27) Shutava, T. G.; Agabekov, V. E.; Lvov, Y. M. Reaction of Radical Cations with Multilayers of Tannic Acid and Polyelectrolytes. *Russ. J. Gen. Chem.* **2007**, *77*, 1494−1501.
(28) Larrauri, J. A.; Sanchez-Moreno, C.; Ruperez, P.; Saura-Calixto, F. Free Radical Scavenging Capacity in the Aging of Selected Red Spanish Wines. *J. Agric. Food Chem.* **1999**, *47*, 1603−1606.
(29) San, N. K.; Kumar, S.; Subramanian, M.; Devasagayam, T. P. A. Variation in the Modulation of Superoxide-Induced Single-strand Breaks in Plasmid PBR322 DNA by Biological Antioxidants. *Biochem. Mol. Biol. Int.* **1995**, *35*, 291−296.
(30) Chen, G. L.; Perchellet, E. M.; Gao, X. M.; Johnson, F. K.; Davis, A. W.; Newell, S. W.; Hemingway, R. W.; Bottari, V.; Perchellet, J. P. Characterization of the Tumor-promoting Activity of m-Chloroperoxybenzoic Acid in SENCAR Mouse Skin and its Inhibition by Gallotannin, Oligomeric Proanthocyanidin, and their Monomeric Units. *Int. J. Oncol.* **1996**, *8*, 197−206.
(31) Lopes, G. K. B.; Schulman, H. S.; Hermes-Lima, M. Polyphenol Tannic Acid Inhibits Hydroxyl Radical Formation from Fenton Reaction by Complexing Ferrous Ions. *Biochim. Biophys. Acta, Gen. Subj.* **1999**, *1472*, 142−152.
(32) Andrade, R. G., Jr.; Dalvi, L. T.; Silva, J. M. C., Jr.; Lopes, G. K. B.; Alonso, A.; Hermes-Lima, M. The Antioxidant Effect of Tannic Acid on the *In Vitro* Copper-Mediated Formation of Free Radicals. *Arch. Biochem. Biophys.* **2005**, *437*, 1−9.
(33) Albu, M. G.; Ghica, M. V.; Giurginca, M.; Trandafir, V.; Popa, L.; Cotrut, C. Spectral Characteristics and Antioxidant Properties of Tannic Acid Immobilized on Collagen Drug-delivery Systems. *Rev. Chim.* **2009**, *60*, 666−672.
(34) Fang, Z. X.; Bhandari, B. Encapsulation of Polyphenols - A Review. *Trends Food Sci. Technol.* **2010**, *21*, 510−523.
(35) Shpigelman, A.; Israeli, G.; Livney, Y. D. Thermally-Induced Protein−polyphenol Co-assemblies: Beta Lactoglobulin-based Nano-complexes as Protective Nanovehicles for EGCG. *Food Hydrocolloids* **2010**, *24*, 735−743.
(36) Oh, H. I.; Hoff, J. E.; Armstrong, G. S.; Haff, L. A. Hydrophobic Interaction in Tannin-Protein Complexes. *J. Agric. Food Chem.* **1980**, *28*, 394−398.
(37) Field, J. A.; Lettinga, G. Toxicity of Tannic Compounds to Microorganisms. In *Plant Polyphenols: Synthesis, Properties, Significance*; Hemingway, R. W., Laks, P. E., Branham, S. J., Eds.; Plenum Press, New York, 1992; pp 673−692.
(38) Meek, K. M.; Weiss, J. B. Differential Fixation of Poly(L-arginine) and Poly(L-lysine) by Tannic Acid and Its Application to the Fixation of Collagen in Electron Microscopy. *Biochim. Biophys. Acta, Gen. Subj.* **1979**, *587*, 112−120.
(39) Liu, M.; Zhang, Y.; Yang, Q.; Xie, Q.; Yao, S. Monitoring and Estimation of the Kinetics Parameters in the Binding Process of Tannic Acid to Bovine Serum Albumin with Electrochemical Quartz Crystal Impedance System. *J. Agric. Food Chem.* **2006**, *54*, 4087−4094.
(40) Stein, W.; Moore, S. Amino Acid Composition of β-Lactoglobulin and Bovine Serum Albumin. *J. Biol. Chem.* **1949**, *178*, 79−71.

DOI: 10.1021/acsami.5b03263
ACS Appl. Mater. Interfaces 2015, 7, 11732−11740

(41) Shutava, T. G.; Balkundi, S. S.; Lvov, Y. M. (−)-Epigallocatechin Gallate/Gelatin Layer-by-Layer Assembled Films and Microcapsules. *J. Colloid Interface Sci.* **2009**, *330*, 276−283.
(42) Carvalho, E.; Mateus, N.; Freitas, V. de. Flow Nephelometric Analysis of Protein-Tannin Interactions. *Anal. Chim. Acta* **2004**, *513*, 97−101.
(43) Labieniec, M.; Gabryelak, T. Interactions of Tannic Acid and Its Derivatives (Ellagic and Gallic acid) with Calf Thymus DNA and Bovine Serum Albumin Using Spectroscopic Method. *J. Photochem. Photobiol., B* **2006**, *82*, 72−78.
(44) Sadovoy, A. V.; Lomova, M. V.; Antipina, M. N.; Braun, N. A.; Sukhorukov, G. B.; Kiryukhin, M. V. Layer-by-Layer Assembled Multilayer Shells for Encapsulation and Release of Fragrance. *ACS Appl. Mater. Interfaces* **2013**, *5*, 8948−8954.
(45) Mo, X.; Shi, M. M.; Huang, J. C.; Wang, M.; Chen, H. Z. Synthesis, Aggregation and Photoconductive Properties of Alkoxycarbonyl Substituted Perylenes. *Dyes Pigm.* **2008**, *76*, 236−242.
(46) Volodkin, D. V.; Larionova, N. I.; Sukhorukov, G. B. Protein Encapsulation via Porous $CaCO_3$ Microparticles Templating. *Biomacromolecules* **2004**, *5*, 1962−1972.
(47) Lomova, M. V.; Sukhorukov, G. B.; Antipina, M. N. Antioxidant Coating of Micronsize Droplets for Prevention of Lipid Peroxidation in Oil-in-Water Emulsion. *ACS Appl. Mater. Interfaces* **2010**, *2*, 3669−3676.
(48) Sadovoy, A. V.; Kiryukhin, M. V.; Sukhorukov, G. B.; Antipina, M. N. Kinetic Stability of Water-Dispersed Oil Droplets Encapsulated in a Polyelectrolyte Multilayer Shell. *Phys. Chem. Chem. Phys.* **2011**, *13*, 4005−4012.
(49) Decher, G. Fuzzy Nanoassemblies: Toward Layered Polymeric Multicomposites. *Science* **1997**, *277*, 1232−1237.
(50) Kiryukhin, M. V.; Gorelik, S. R.; Man, S. M.; Subramanian, G. S.; Antipina, M. N.; Low, H. Y.; Sukhorukov, G. B. Individually Addressable Patterned Multilayer Microchambers for Site-Specific Release-on-Demand. *Macromol. Rapid Commun.* **2013**, *34*, 87−93.
(51) Kern, W. The Evolution of Silicon Wafer Cleaning Technology. *J. Electrochem. Soc.* **1990**, *137*, 1887−1892.
(52) Guo, X.; Liu, L.; Wang, W.; Zhang, J.; Wang, Y.; Yu, S.-H. Controlled Crystallization of Hierarchical and Porous Calcium Carbonate Crystals Using Polypeptide Type Block Copolymer as Crystal Growth Modifier in a Mixed Solution. *CrystEngComm* **2011**, *13*, 2054−2061.
(53) Garnier, A.; Tosi, L. Cu(II)-Poly(L-arginine) Complexes. Potentiometric and Spectral Characterization of Amine and Peptide Nitrogen Ligands. *Biopolymers* **1975**, *14*, 2247−2262.
(54) McDonald, M.; Mila, I.; Scalbert, A. Precipitation of Metal Ions by Plant Polyphenols: Optimal Conditions and Origin of Precipitation. *J. Agric. Food Chem.* **1996**, *44*, 599−606.
(55) South, P. K.; Miller, D. D. Iron Binding by Tannic Acid: Effects of Selected Ligands. *Food Chem.* **1998**, *63*, 167−172.
(56) Barbosa, L. R. S.; Ortore, M. G.; Spinozzi, F.; Mariani, P.; Bernstorff, S.; Itri, R. The Importance of Protein-Protein Interactions on the pH-Induced Conformational Changes of Bovine Serum Albumin: A Small-Angle X-Ray Scattering Study. *Biophys. J.* **2010**, *98*, 147−157.

DOI: 10.1021/acsami.5b03263
ACS Appl. Mater. Interfaces 2015, 7, 11732−11740